

## Characteristic and continuum x rays produced with potassium ions of a few MeV

Louis Brown, G. E. Assousa, and Norbert Thonnard

*Department of Terrestrial Magnetism, Carnegie Institution of Washington, Washington, D. C. 20015*

H. A. Van Rinsvelt

*Department of Physics and Astronomy, University of Florida, Gainesville, Florida 32611*

Cidambi K. Kumar

*Department of Physics and Astronomy, Howard University, Washington, D. C. 20001*

*and Department of Terrestrial Magnetism, Carnegie Institution of Washington, Washington, D. C. 20015*

(Received 4 November 1974; revised manuscript received 21 April 1975)

We report observations of x radiation from 1.0 to 4.5 keV produced by the collision of  $K^+$  ions of 0.5 to 3.0 MeV with thick targets. Characteristic lines of the beam or the target or both are observed, depending on the target. These lines are superimposed on a continuum that is exponential in form. The relative dependence of the line yields on atomic number and the continuum on photon energy can be reproduced without the use of an adjustable parameter, if one assumes that the processes are controlled by the Fourier spectrum experienced by an orbital electron that results from the passage of a uniformly moving charged particle. A mechanism is proposed that allows this control to function in producing  $K$ -shell vacancies. The formulas are applied to other data and are shown to reproduce the relative  $Z$  dependence for projectiles of 0.01 to 2.5 MeV/amu with  $Z_1$  ranging from 17 to 82.

### I. INTRODUCTION

The collision of potassium ions of a few MeV with targets of arbitrary atomic number is a good experiment for examining the production of x rays that result from the interpenetration of electron shells. In particular it allows the study of nearly matched  $K$  shells, where the mechanism for creating vacancies is obscure, and it allows the study to be made under conditions where Coulomb excitation is negligible. In addition to the characteristic x-ray lines, a continuum has been discovered,<sup>1,2</sup> which has been interpreted as the result of transitions to vacancies in the molecular orbitals while the colliding atoms are in close proximity.

Electron promotion<sup>3,4</sup> from the  $2p\sigma$  to the  $1s\sigma$  molecular orbital has been the obvious model for interpreting these collisions, as it has had many successes, but its application to deep encounters with nearly matched  $K$  shells has led to a contradiction for atoms of atomic number greater than 10 if the heavier partner enters the collision without vacancies in the  $2p$  shell. Theories in which the Coulomb force produces the required holes through direct interaction on the  $K$  shell have not been developed for collisions between atoms of comparable atomic number, but all indications are that they fail by orders of magnitude to predict the cross section. Recently Meyerhof and co-workers<sup>5,6</sup> have suggested that  $K$ -vacancy formation occurs by direct Coulomb excitation from the  $1s\sigma$  and  $2p\sigma$  orbitals to high-lying vacant or con-

tinuum states.

We shall demonstrate that our measurements and those of others as well show evidence that the processes are controlled by the Coulomb interaction of the moving nucleus but that they are probably not due to direct interactions. Recent proposals to explain the photon energy dependence of the molecular-orbital continuum use stimulated radiative transitions.<sup>7-9</sup> Our method of describing the interaction handles this well and suggests that inner-shell vacancy production may also result from induced transitions.

### II. EXPERIMENT AND APPARATUS

We observed the x-ray spectra produced by a beam of singly ionized potassium hitting thick targets. Somewhat arbitrarily we selected the energy range of the spectrum to extend from 1 to 4.5 keV. This range included the  $K$  lines of potassium and a portion of the continuum. Photons below 1 keV lie outside the range of our detector. Thus, for characteristic lines, the experiment dealt with  $K$  lines from the beam plus whatever  $K$ ,  $L$ , or  $M$  lines from the target fell within the selected energy range of the detector.

The beams of potassium ions originated in a hot-wire ionizer, so that ions were produced from atoms with very low ionization potentials. The Carnegie pressure-tank Van de Graaff machine accelerated them. The analyzing magnet allows a deflection of only  $7^\circ$ , and beam purity at the source is important. The charged-particle spectrum dis-

closed by the magnet showed monoenergetic lines only for alkali metals and convinced us that multiply charged rubidium was the only contaminant. This resulted from the traces of rubidium in the KCl charge of the ion source that were further ionized by the collision with the residual gas of the tube. We estimated the rubidium to be present in the deflected beam at the target in amounts of at most a few parts per hundred thousand.

A thick target intercepted the beam at  $45^\circ$  and was viewed by a Si(Li) detector mounted on the target chamber with a vacuum connection at  $90^\circ$  to the beam. The only attenuation between the target and the detector crystal was a 0.025 mm beryllium window, although in some cases a Mylar foil was added to attenuate further the low-energy photons. The data were corrected for absorption by the window by an empirical formula.<sup>10</sup> No correction nor calibration was made for the low-energy portion of the spectrum where losses in the gold electrode and the dead layer occur.

The accurate determination of the yield of photons per unit charge of the beam entails experimental problems. (i) A large flux of electrons and photons leaves the target; the photons release copious numbers of photoelectrons from the walls of the chamber with the result that these effects cannot be corrected with target bias. We insulated the entire chamber, which had only small apertures for the entrance of the beam and exit of the photons to the detector, and integrated the total current from the chamber. (ii) The portion of the beam that does not pass into the chamber and strikes the beam tube preceding it releases large numbers of electrons that can enter the chamber, and are even guided into it by the positively charged beam; similarly, electrons from the chamber can escape by the same route. We placed a series of apertures before the insulated target chamber and a magnetic field across the region, which reduced these effects to a negligible amount. (iii) The residual gas of the beam tube in the region between the analyzing magnet and the target chamber can ionize the singly charged beam to higher-charge states, giving an incorrect measure of the number of incident ions. We pumped this tube with a cold trapped diffusion pump and corrected our data for the indicated pressure. This correction, which was never more than 20%, is not very good and is a source of error. (iv) Carbon buildup reduces the energy of the beam and contributes to the error through the strong energy dependence of the thick-target yields. We measured its effect and moved the target occasionally to reduce its effect to negligible size. (v) Potassium buildup in the target gives errors, if one is observing the potassium lines. We found that the precautions needed to

prevent carbon buildup sufficed to prevent this. The target was kept out of the beam except when needed. (vi) The pulse amplifier had some difficult count-rate problems, the effect of the large flux below 1 keV being particularly troublesome. We ran at the lowest count rates that were practical, but even with this precaution, it was probably our greatest source of error and one of uncertain magnitude. The pulse-height analyzer gated the current integrator during its dead time and presented no problems in this regard.

The potassium beam is not suitable for examining the targets for impurities because of the strong  $Z$  dependence of the excitation mechanism. We bombarded the targets with 1 MeV protons and observed the x radiation from 1 to 22 keV produced, thereby identifying impurities as well as confirming the atomic number of each target.

### III. EXPERIMENTAL RESULTS

Three spectra are shown in Fig. 1 that are typical of the measurements. Characteristic lines are seen superimposed on an x-ray continuum of approximately exponential form. The three examples result from a 2.00 MeV  $K^+$  beam incident on thick targets of aluminum, yttrium, and iron, noted, respectively, according to the location of the peaks from left to right. For the first two the potassium  $K$  shell has a greater binding energy than the aluminum  $K$  or the yttrium  $L$  shell, both of whose lines stand out; in both cases the potassium  $K$  lines are barely discernible. In the third spectrum the potassium  $K$  shell has a smaller binding energy than the iron  $K$  shell; the potassium lines stand out, and the iron  $K$  lines, although outside the energy range of the spectrum reproduced here, were looked for and found to be much less intense. This swapping effect is well established,<sup>3</sup> and we observe it for  $K$ ,  $L$ , and  $M$  shells that nearly overlap the  $K$  shell of potassium. The yields of the characteristic lines observed are shown in Fig. 2 for a 2.00 MeV beam. The  $K$  lines from the beam are shown as solid circles, radiation from the target as open circles. The range of atomic number where the  $K$  shell of potassium overlaps a shell of the target is shown with shading.

The continua for the range of  $Z = 13$  through  $Z = 32$  are very similar in shape. In some cases there is evidence of target impurities, but for targets of atomic number 21, 22, 23, 26, and 27 the results can be fitted to an exponential over the range from 1.2 to 2.3 keV. The parameters are given in Table I. The continua for targets with atomic number greater than 40 follow the same shape but do not allow the regular exponential description. All of the data

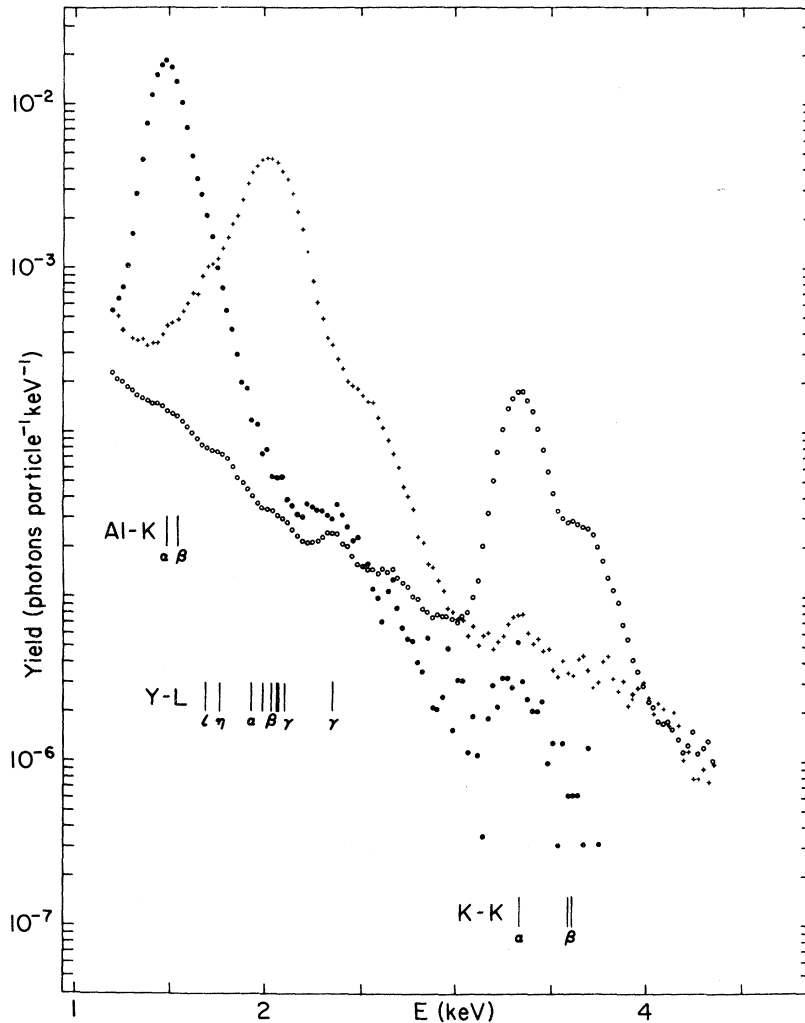


FIG. 1. Examples of spectra obtained by bombarding three different targets with  $K^+$  at 2.00 MeV. The spectrum having the leftmost peak is from an aluminum target; the aluminum  $K$  lines are strong and there is only a suggestion of potassium  $K$  lines. The spectra having the rightmost peak is from an iron target; the potassium  $K$  lines are strong; the iron  $K$  lines fall outside the plot but are known to be very weak. The spectrum with the peak at left center is from a yttrium target; the yttrium  $L$  lines are strong and the potassium  $K$  lines are very weak. The unperturbed locations of the various lines are indicated. These lines were used to establish the energy scale, so energy shifts cannot be read from their positions.

in this latter region have greater amounts of error owing to the large flux of photons below 1 keV, many of which pass the beryllium window and for which the compensation made by reducing the counting rate was not enough.

We also bombarded reactor-grade graphite. One would expect that the carbon nucleus would ionize the potassium  $K$  shell through Coulomb excitation, and we did see these lines. The graphite showed a strong line at 2.65 keV and two weak ones at 1.8 and 2.3 keV. Proton bombardment confirmed that these lines result from Cl, Si, and S. The yield of the potassium lines was not reproducible and much larger than the value calculated from Coulomb excitation,<sup>11</sup> so we attribute it to excitation by impurities, as the proton bombardment disclosed considerable Ca and Fe and some Ti and V. The graphite showed a smooth continuum from 1.0 to 1.5 keV. We observed the continuum from a 20  $\mu\text{g}/\text{cm}^2$  thick carbon foil, which showed the

same contaminants as the thick target but also the same smooth region of continuum. The results for the continuum are given in Fig. 3.

The yields of the potassium  $K$  lines as functions of incident particle energy were measured for targets just beyond potassium in atomic number; the results are shown in Fig. 4. Errors from impurities were negligible for all these targets.

#### IV. INTERPRETATION

Coulomb excitation or direct interaction, calculated by means of the Born, binary encounter, or semiclassical approximations, is the only successful theory to account for the production of holes in the inner shells of atoms in heavy-ion collisions. Its validity requires that either the ionizing particle have no electrons or those that it has have much smaller binding energies than the shells wherein the holes are to be produced, conditions that are not met in this experiment. Meyerhof and

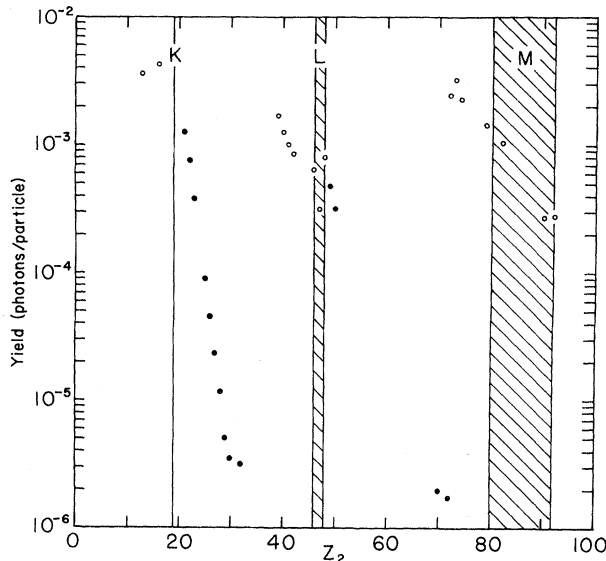


FIG. 2. Thick-target yield of x rays observed in the photon energy range 1.0–4.5 keV produced with a 2.00-MeV  $K^+$  beam. The open circles are data points for radiation from the target: for  $10 < Z < 20$  they are  $K$  lines, for  $35 < Z < 50$  they are  $L$  lines, for  $Z > 70$  they are  $M$  lines. The solid circles are points for the  $K$  lines of potassium. The lower limit of observation for these lines is determined by the continuum. The shaded regions show the range of targets whose  $L$  or  $M$  shells overlap the  $K$  shell of potassium. The atomic numbers of the targets are 13, 16, 21–23, 25–30, 32, 39–42, 46–50, 70, 72–74, 79, 82, 90, 92.

co-workers<sup>5,6</sup> have proposed that excitation from the  $1s\sigma$  and  $2p\sigma$  orbital to vacant states higher than the  $2p\pi$  orbital or to the continuum produces  $K$  vacancies, thereby avoiding the difficulties of electron promotion. They call this process Coulomb excitation from molecular orbital and investigate its plausibility through scaling attempts. For symmetric collisions they find that the experimental

TABLE I. The photon yield  $Y(1.5)$  at 1.5 keV in photons  $\text{keV}^{-1}\text{particle}^{-1}$  for the x-ray continua from 1.2 to 2.3 keV that result from 2.00-MeV  $K^+$  ions incident on solid targets of atomic number  $Z_2$ , described by  $Y(E) = Y(1.5) \times \exp[-2.4(E - 1.5)]$ , where  $E$  is the photon energy in keV.

$Z_2$	$10^4 Y(1.5)$
21	5.1
22	3.7
23	2.6
26	1.2
27	0.82

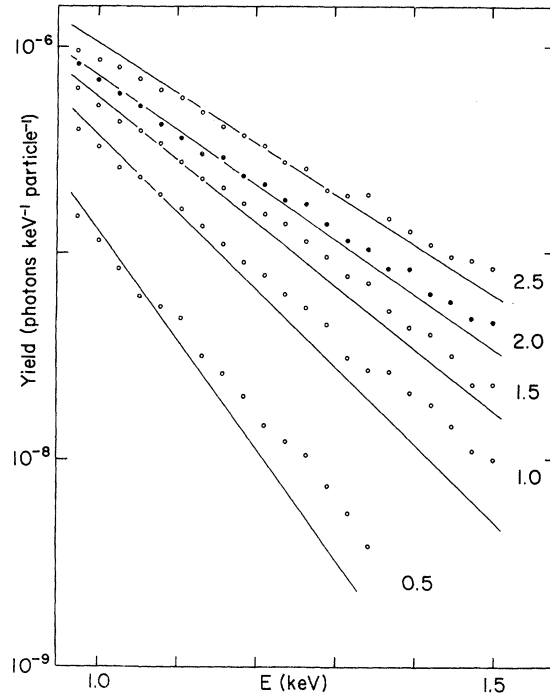


FIG. 3. X-ray continua resulting from potassium ions of 0.5 to 2.5 MeV striking a  $20 \mu\text{g}/\text{cm}^2$  carbon foil. Solid and open circles distinguish nearby sets of data. Beyond 1.5 keV impurities in the foil obscured the continuum; below 1.0 keV the correction for the beryllium window of the detector is too large for reliable application. The straight lines are calculated from the exponential of Eq. (7) with  $n=2$ .

summed target and projectile cross section for  $Z_1, Z_2 > 10$  with gaseous targets and for  $Z_1, Z_2 \geq 50$  with solid targets is given by the approximate empirical formula

$$\sigma = \frac{1}{4} \left( \frac{1}{Z_1} + \frac{1}{Z_2} \right)^2 \frac{63 \xi_0^{4.3}}{1 + 10^{-5} \xi_0^{-4} + 1.8 \times 10^{-10} \xi_0^{-8}} \pi a_0^2 \quad (1)$$

where

$$\xi_0 = \left( \frac{E_1 m}{M_1 U} \right)^{1/2} \quad (2)$$

with  $E_1$  and  $M_1$  being the projectile energy and mass,  $U$  is the binding energy of the  $2p\sigma$  at the distance of closest approach,  $m$  is the electron mass, and  $a_0$  is the Bohr radius. They find Eq. (1) gives a poorer fit to the asymmetric than to the symmetric collision data. We shall apply this formula to our data for comparison but have also gone into the matter from another, but not necessarily conflicting, point of view. We have sought a scaling law that can correlate the data and have

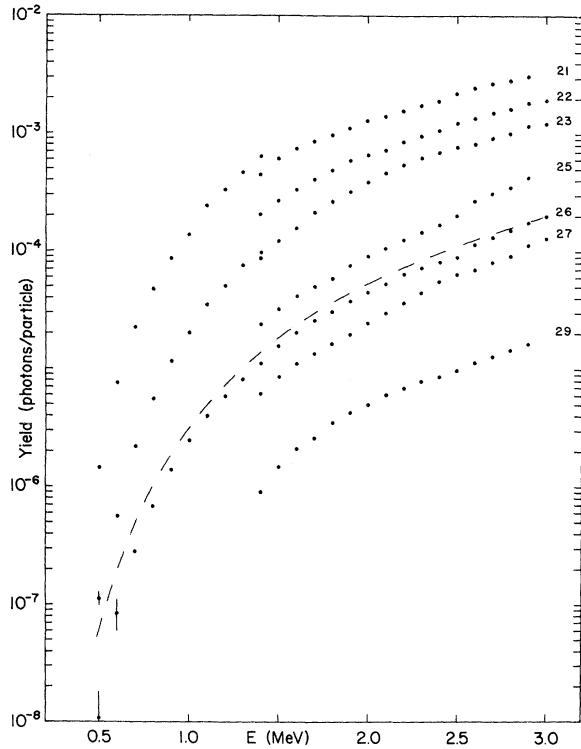


FIG. 4. Thick-target yields of the potassium  $K$  lines as functions of the ion energy for various targets. Numbers at the right are  $Z_2$ . The failure of some data to match at 1.4 MeV, which separates data taken on different days, and probably some of the irregularities result from the sources of error listed in Sec. II. The dashed curve is thick-target yield calculated from Eq. (1) of Meyerhof *et al.*<sup>5</sup> and normalized to the data at projectile energy of 3 MeV.

found the Fourier spectrum of a moving charged particle useful.

The time varying electric field experienced by an orbital electron that results from the passage of a moving charged particle is a likely cause of vacancy production, as it is for the direct interaction process. From a general point of view consider the amplitude of frequencies in the Fourier spectrum of the time varying field produced by a uniformly moving particle. This field is

$$\mathcal{E}(t) = Ze / (p^2 + v^2 t^2), \quad (3)$$

where  $p$  is the perpendicular distance from the field point and the straight-line trajectory of the projectile of charge  $Ze$  and velocity  $v$ . The Fourier transform gives the spectrum of virtual photons to be

$$I(E) = \frac{Ze}{2\hbar p v} \exp\left(-\frac{E p}{\hbar v}\right), \quad (4)$$

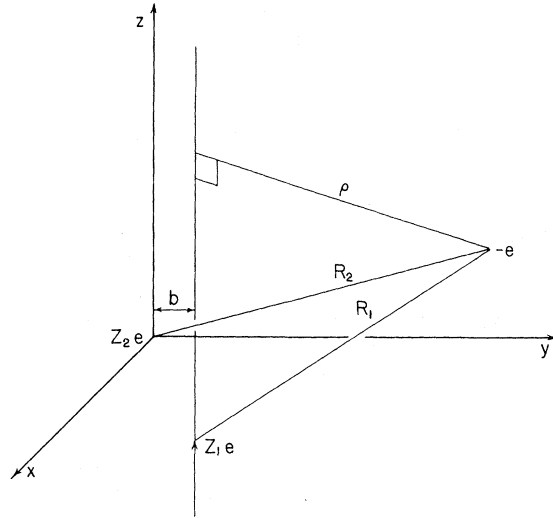


FIG. 5. Geometry for use with Eqs. (3), (4), and (5). The target nucleus is located at the center of the coordinate system  $x, y, z$ ; the projectile nucleus moves in a straight line in the  $y-z$  plane, parallel to the  $z$  axis, and at a distance  $b$  from it. The cylindrical coordinate  $\rho$  locates the electron position relative to the path of the projectile.

if we replace the circular frequency through the Planck relationship  $\omega = E/\hbar$ , where  $E$  is the energy of the virtual photon.

In applying this spectrum to a heavy-ion collision we assume the distance parameter  $p$  to be proportional to the expectation value of the cylindrical coordinate  $\rho$ , as shown in Fig. 5. We further assume that the excitation occurs when the two nuclei pass well within the  $K$  shell of the united atom; therefore, the impact parameter  $b$  is much less than the  $K$ -shell radius, so we take

$$p_n \propto \int_v \Psi_n^* \rho \Psi_n dV, \quad (5)$$

where  $\Psi_n$  is the wave function of an electron trying to form a united-atom shell of principal quantum number  $n$ . Ignorance of  $\Psi_n$  lies at the heart of the problem of heavy-ion collisions, but it seems reasonable to assume that Eq. (5) will be proportional to  $r_n$ , the expectation value of the radius for the united atom. If we use the expectation value from the hydrogenic atom for  $n=1$  or  $2$  with  $l=0$  we find, in fact, that the constant of proportionality is very nearly unity and hence choose  $p_n = r_n$  for all of the comparisons to be made here.

If we consider the ejection of a  $2p$  electron from the united atom, thereby creating the required vacancy in the  $2p\sigma$  orbital, by some process related to  $I(E)$ , we set  $E$  equal to the hydrogenic atom

binding energy and  $p$  equal to the expectation value of  $r$  for the  $n=2$  shell of the united atom. Equation (3) becomes for arbitrary  $n$

$$I_n(Z_2) = \frac{Z(Z_1+Z_2)e}{3n^2 a_0 \hbar v} \exp\left(-\frac{3}{4} \frac{e^2(Z_1+Z_2)}{\hbar v}\right). \quad (6)$$

The value of  $Z$  to use will be an effective one whose selection is complicated by the relative motion, but it does not appear in the argument of the exponential, which dominates Eq. (6). Screening, which might be introduced to improve the accuracy of the hydrogenic atom formulas, will not affect the use of Eq. (6), as we apply it only to relative changes in  $Z_2$ .

There is independent evidence<sup>7-9</sup> that the molecular-orbital continuum radiation is stimulated and Eq. (4) should serve as an approximation of the stimulating field with the same interpretation in meaning for  $p_n$  as applied to the production of holes in the  $2p\sigma$  orbital. Equation (4) becomes

$$I_n(E, Z_2) = \frac{Z(Z_1+Z_2)e}{3n^2 a_0 \hbar v} \exp\left(-\frac{3n^2 a_0 E}{2 Z_1+Z_2 \hbar v}\right). \quad (7)$$

We shall now make comparisons of the relative yields or cross sections of our own data and those of others available to us using Eq. (1) from Meyerhof and co-workers and our own arguments, Eqs. (6) and (7). Equation (1) predicts absolute values, but Eqs. (6) and (7) do not. We shall compare results only with the exponential of these latter two equations, as we do not know what value to give  $Z$ ; the errors introduced by this are small when compared with the large variation of the data and of the exponential.

In Fig. 6 are shown the relative  $Z_2$  dependences of  $K^+$  for four energies with various targets. The predictions of Eq. (1) are shown with dashed lines for the highest and lowest energies, those of Eq. (6) are shown with full curves for all energies. Equation (6) is incapable of correlating the dependence of yield with projectile energy, whereas Eq. (1) does this quite well, as shown in Fig. 4. We have made arbitrary normalizations in all of these comparisons, although Eq. (1) is fairly good for  $Z_1=Z_2=19$ . The agreement of Eq. (1) for varying projectile energy is not surprising, when one considers that its origin lies in a fit to these kinds of data.

A considerable range of measurements is available for the relative  $Z_2$  dependence with projectiles of  $Z_1$  comparable to  $Z_2$ . In Fig. 7 are shown all measurements<sup>5,6,12-14</sup> known to us at the time of this writing. Calculations from Eq. (1) are shown as dashed curves; normalizations were required but they are small on the scale of the graph. Cal-

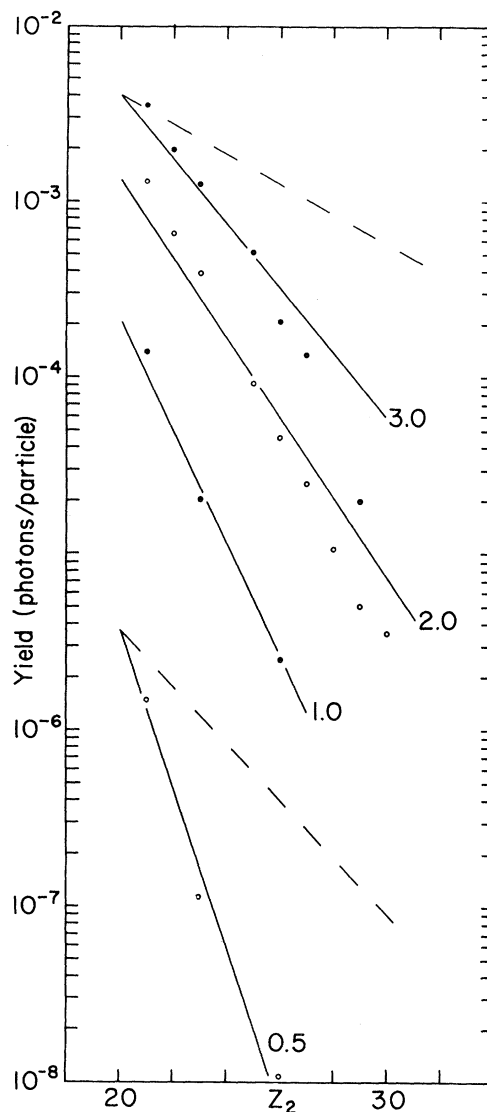


FIG. 6. Thick-target yields of potassium  $K$  lines as functions of the target atomic number for four values of projectile energy. Solid and open circles distinguish nearby sets of data. The numbers at the right are projectile energies in MeV. The dashed curves are calculated from Eq. (1) and solid curves are from the exponential portion of Eq. (6), both normalized to the data at  $Z_2=20$ .

culations from Eq. (6) are shown as full lines and have arbitrary normalization. Note that Figs. 6 and 7 show data with projectile energies ranging from 0.013 to 2.5 MeV/amu and projectile atomic numbers from 17 to 82.

Our measurements of x-ray continua are shown in Figs. 1 and 3. If these continua result from transitions to vacancies in the molecular orbitals, then they are certainly associated not with transi-

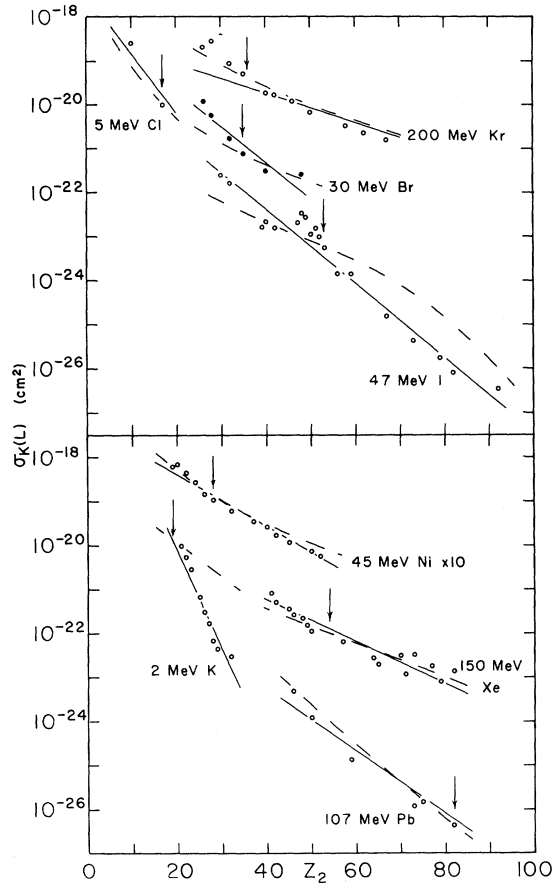


FIG. 7. Cross sections for  $K$  vacancy production as function of  $Z_2$  for eight experiments. The value given is the sum of projectile and target cross sections, which is in effect the cross section for the light collision partner. Solid and open circles distinguish nearby data. Projectile energy and kind are indicated for each group. Vertical arrows indicate  $Z_1$ . The 2-MeV  $K$  points are from the present work; the 5-MeV  $Cl$  are from Ref. 12; the 45-MeV  $Ni$  are from Ref. 13; the 150-MeV  $Xe$  are from Ref. 14; and the remainder are from Ref. 6. The dashed curves are from Eq. (1) with small normalization adjustment; the solid curves are from the exponential portion of Eq. (6) with arbitrary normalization.

tions filling vacancies in the  $1s\sigma^{2,3}$  ( $K$  band) but with those filling the  $2s\sigma$ ,  $2p\pi$ , or  $2p\sigma^{15}$  ( $L$  band). They cannot result from nucleus-nucleus bremsstrahlung because the intensities are too high and the  $Z$  dependence is opposite the prediction. In the case of the results shown in Fig. 3,  $K^+ + C$ , the shell on which the series terminates would be the united-atom  $2p$  shell, which has an energy of 0.77 keV. To see this band beyond this limit is explained by the broadening of the levels owing to the short collision times. Indeed a distinctive cutoff is also not observed for the  $K$  band.<sup>7</sup>

In Fig. 3 is shown the exponential part of Eq. (7) with  $n=2$  for various values of projectile energy. In Fig. 8 we apply Eq. (7) to our own  $K^+ + V$  data and to representative continuum data of others<sup>16,17</sup> that were available to us. We have used only measurements that have been corrected by the authors for detector efficiency and window absorption. Four cases of  $K$  and one of  $L$  band are shown with  $n=1$  used for the former and  $n=2$  for the latter.

Meyerhof *et al.*<sup>16</sup> have proposed a theory for the spectrum of the molecular orbital continuum, which reproduces the shape and magnitude of the  $K$  band. It assumes the transitions are spontaneous, although recent experiments<sup>7-9</sup> show evidence that induced transitions are important. We have not applied it to our continua as it requires for the  $K$  band the calculation of the transfer of vacancies from the  $2p\sigma$  to the  $1s\sigma$  orbital, a mechanism whose parallel for the  $L$  band is difficult to calculate.

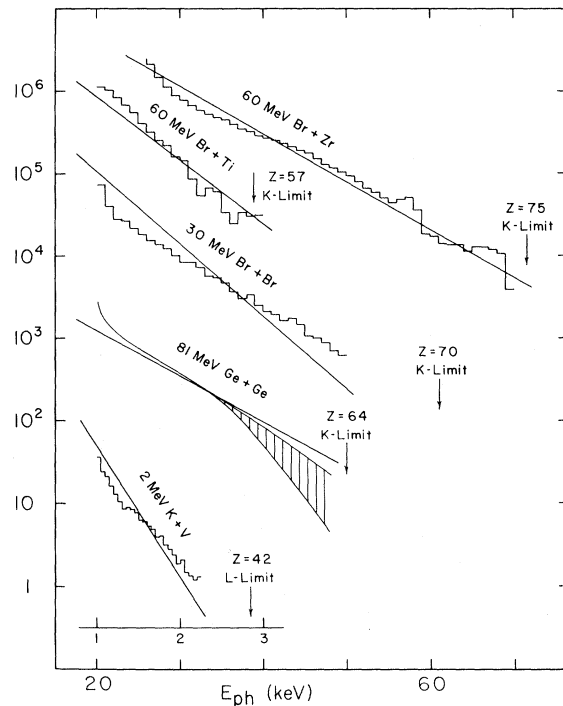


FIG. 8. X-ray continuum yield per unit energy interval in arbitrary units as a function of photon energy. Vertical arrows indicate the united-atom limit. The top three measurements are from Ref. 16, the fourth, which has pulse-height-analyzer points reproduced by a curve and a shaded region, is from Ref. 17, and the bottom, which has a different (1-3 keV) energy scale from the other four, is from the present work. The straight lines are from the exponential portion of Eq. (7) with  $n=2$  for the 2-MeV  $K$  on  $V$  and  $n=1$  for the others.

The two equations derived from the Fourier spectrum of a uniformly moving charged particle reproduce within the accuracy of the data the relative  $Z_2$  dependence of the vacancy production in the  $2p\sigma$  orbital and the  $E$  dependence of what we presume to be the molecular orbital continuum. In the case of the continuum the relationship of  $I_n(E, Z_2)$  to the data suggests stimulated transitions. In the case of the  $2p\sigma$  vacancies we have demonstrated the ability of  $I_n(Z_2)$  to correlate cross section with the amplitude of the Fourier spectrum at the frequency required to eject the electron, but a mechanism by which this proceeds is not apparent.

The question arises as to whether Eq. (6) also works in regions where direct interaction theory describes the results accurately. We find that it not only fails but fails in a manner that can be removed only by making the relation between  $p_n$  and  $r_n$  a function of  $Z_2$  and  $v$ , which removes any utility the formula may have.

The mechanism proposed by Meyerhof and co-workers<sup>5,6</sup> may be compatible with Eq. (6) and the failure of Eq. (1) to reproduce the  $Z_2$  dependence of our data cannot be taken as a contradiction of the mechanism they propose, as their theory is at the stage of a plausibility argument derived from symmetric collisions and does scale most of the data presented in Fig. 7 fairly well. Nevertheless, the ability of Eq. (6) to give the  $Z$  dependence of data having such a wide range of energy and atomic number together with its failure to give the dependence where Coulomb excitation works, leads us to propose another heretofore unconsidered mechanism.

If holes in the  $2p\sigma$  orbital are produced through an induced transition, then the proportionality of the cross section with  $I_n(Z_2)$  would make sense, and a radiationless transition by an electron more tightly bound than the  $2p\sigma$  seems to be a possibility worth considering. Figure 9 has a plot of the energies of the  $2p\sigma$  and  $1s\sigma$  molecular orbitals as functions of the internuclear distance for K + Sc made by estimated scaling of Ar + Ar calculations.<sup>18</sup> The abscissa plots distance and time, related through the ion velocity, the ordinate plots energy and electron oscillation frequency. The calculations assume the transformation to be adiabatic, which requires that

$$\frac{\tau}{E_i - E_f} \frac{\partial U}{\partial t} \ll 1, \quad (8)$$

where  $\tau$  is the electron oscillation period,  $E_i$  and  $E_f$  are the initial and final energies, and  $\partial U/\partial t$  is the rate of change of potential energy. The sudden approximation requires the reverse inequality. For this experiment conditions for the application

of both the slow and fast approximations are about equally badly satisfied.

We are unable to calculate the behavior of the electrons trying to follow the  $1s\sigma$  orbital under these conditions, but it seems reasonable that they may undergo quantum jumps in trying to form the  $1s$  shell of the united atom. The binding energy of the  $2p\sigma$  is small compared with the total change required of the  $1s\sigma$  electrons, so radiationless quantum jumps could release sufficient energy to eject a  $2p\sigma$  electron. Estimates of the spontaneous transition lifetimes for static conditions are long compared with the collision times, implying that induced transitions should be important. Looking at the matter from another point of view, one might expect the results to be similar to what would happen if the nuclear charge of either atom were changed abruptly to  $Z_1 + Z_2$ . In  $\beta$  decay, increases of atomic number from  $Z$  to  $Z + 1$  cause holes to be created in all shells.<sup>19</sup> The penetration of the light nucleus into the  $K$  shell of the heavy can also be viewed as an increase—and a large one—of the nuclear charge, thereby giving rise to large shake-off effects.

Our measurements also include target  $L$  and  $M$

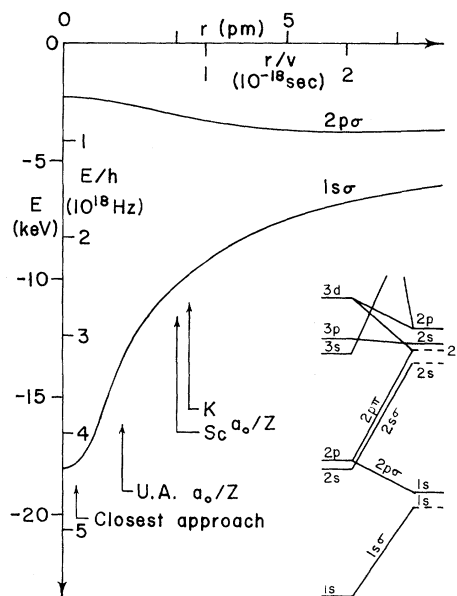


FIG. 9. Energy levels of the diatomic system K + Sc. In the lower right is the correlation diagram for the inner shells. The united-atom structure is at the left; the separated-atom structures are at the right with Sc denoted with dashed and K with solid lines. The remainder of the figure shows the energies of the  $1s\sigma$  and  $2p\sigma$  molecular orbitals as functions of the internuclear separation, which has been converted to units of time through the ion velocity.



x rays produced by the near overlap of those shells with the  $K$  shell of potassium, as seen in Fig. 2. The mechanism proposed should function there as well, but the matter will not be as clear cut as it is for  $K$ -shell emission, because there is considerable evidence that electron promotion occurs.<sup>3,4</sup> Equation (6) predicts a stronger  $Z$  dependence than is observed. This deviation could be attributed to the contribution of electron promotion or to the breakdown of Eq. (6) when applied to the  $n=3$  and 4 shells of the united atom. We have also been unsuccessful in fitting the continua in these two regions and suspect Eq. (7) breaks down for the  $M$  and  $N$  bands.

### V. CONCLUSIONS

We report measurements of the yields of characteristic x-ray lines and continua produced by a potassium beam of a few MeV incident on a variety of targets. The conditions of the experiment are such that direct Coulomb interaction is not expected to apply and electron promotion is unable to fit. These observations together with the results of experiments reported elsewhere receive quantitative fit of the  $Z_2$  dependence of the line data and the  $E$  dependence of the continuum data, both without the use of an adjustable parameter, if the transitions are assumed to take place in proportion to the amplitude of the Fourier spectrum (at the frequency of the transition) characterizing the passage of the projectile nucleus. This suggests

that the Coulomb interaction controls both the production of the  $K$ -shell vacancies and the shape of the x-ray continuum. We propose a mechanism for vacancy production that uses this spectrum through stimulated Auger transitions, thereby extracting energy from the electrons trying to form the  $1s\sigma$  orbital to eject a  $2p\sigma$  electron rather than extracting the energy from the field of virtual photons.

The deficiencies of Eqs. (6) and (7) are evident, for they do not constitute a theory of the processes they describe and are only one step removed from empirical formulas. Nevertheless, their origin lies in such simple ideas and their accuracy as scaling laws is sufficiently high that they may offer a clue to the explanation of these two puzzling phenomena.

### VI. ACKNOWLEDGMENTS

We wish to thank Werner Brandt and his colleagues for their discussions and Walter E. Meyerhof for his discussions and for sending us the details of the work done by him and his co-workers in advance of publication, which included most of the data shown in Fig. 7. George H. Pepper taught us about direct interaction theories and his criticisms led us to remove from the text parts that would have pained us later. Chris Soares did the analysis of the targets with protons from the Van de Graaff machine of the University of Florida; we are pleased to acknowledge his help and thank him here.

<sup>1</sup>F. W. Saris, W. F. van der Weg, H. Tawara, and R. Laubert, *Phys. Rev. Lett.* **28**, 717 (1972).

<sup>2</sup>W. E. Meyerhof, T. K. Saylor, S. M. Lazarus, A. Little, B. B. Triplett, and L. F. Chase, Jr., *Phys. Rev. Lett.* **30**, 1279 (1973).

<sup>3</sup>M. Barat and W. Lichten, *Phys. Rev. A* **6**, 211 (1972).

<sup>4</sup>J. D. Garcia, R. J. Fortner, and T. M. Kavanagh, *Rev. Mod. Phys.* **45**, 111 (1973).

<sup>5</sup>W. E. Meyerhof, *Phys. Rev. A* **10**, 1005 (1974).

<sup>6</sup>W. E. Meyerhof, T. K. Saylor, S. M. Lazarus, A. Little, B. B. Triplett, R. Anholt, L. F. Chase, Jr., and P. D. Bond (private communication).

<sup>7</sup>J. S. Greenberg, C. K. Davis, and P. Vincent, *Phys. Rev. Lett.* **33**, 473 (1974).

<sup>8</sup>G. Kraft, P. H. Mokler, and H. J. Stein, *Phys. Rev. Lett.* **33**, 476 (1974).

<sup>9</sup>R. S. Thoe, I. A. Sellin, M. D. Brown, J. P. Forester, P. M. Griffin, D. J. Pegg, and R. S. Peterson, *Phys. Rev. Lett.* **34**, 64 (1975).

<sup>10</sup>M. C. Lambert and A. Engström, in *Handbook of X-Rays*, edited by E. F. Kaelble (McGraw-Hill, New York,

1967).

<sup>11</sup>W. Brandt, R. Laubert, and I. Sellin, *Phys. Rev.* **151**, 56 (1966).

<sup>12</sup>L. Winters, M. D. Brown, L. D. Ellsworth, T. Chiao, E. W. Pettus, and J. R. Macdonald, *Phys. Rev. A* **11**, 174 (1975).

<sup>13</sup>H. Kubo, F. C. Jundt, and K. H. Purser, *Phys. Rev. Lett.* **31**, 674 (1973).

<sup>14</sup>P. Gippner, K. H. Kaun, W. Neubert, F. Stary, and W. Schulze, *Nucl. Phys. A* **245**, 336 (1975).

<sup>15</sup>G. Bissinger and L. C. Feldman, *Phys. Rev. Lett.* **33**, 1 (1974).

<sup>16</sup>W. E. Meyerhof, T. K. Saylor, S. M. Lazarus, A. Little, B. B. Triplett, L. F. Chase, Jr., and R. Anholt, *Phys. Rev. Lett.* **32**, 1279 (1974).

<sup>17</sup>P. Gippner, K. H. Kaun, F. Stary, W. Schulze, and Yu. P. Tretyakov, *Nucl. Phys. A* **230**, 509 (1974).

<sup>18</sup>U. Fano and W. Lichten, *Phys. Rev. Lett.* **14**, 627 (1965); W. Lichten, *Phys. Rev.* **164**, 131 (1967).

<sup>19</sup>B. Crasemann and P. Stephas, *Nucl. Phys. A* **134**, 641 (1969).